

Nuclear structure corrections to the Lamb shift in $\mu^3\text{He}^+$ and $\mu^3\text{H}$

N. Nevo Dinur,^{1,*} C. Ji,^{2,3,4,†} S. Bacca,^{2,5,‡} and N. Barnea^{1,§}

¹*Racah Institute of Physics, The Hebrew University, Jerusalem 91904, Israel*

²*TRIUMF, 4004 Wesbrook Mall, Vancouver, BC V6T 2A3, Canada*

³*ECT*, Villa Tambosi, 38123 Villazzano (Trento), Italy*

⁴*INFN-TIFPA, Trento Institute for Fundamental Physics and Applications, Trento, Italy*

⁵*Department of Physics and Astronomy, University of Manitoba, Winnipeg, MB, Canada R3T 2N2*

(Dated: December 18, 2015)

Measuring the 2S-2P Lamb shift in a hydrogen-like muonic atom allows one to extract its nuclear charge radius with a high precision that is limited by the uncertainty in the nuclear structure corrections. The charge radius of the proton thus extracted was found to be 7σ away from the CODATA value, in what has become the yet unsolved “proton radius puzzle”. Further experiments currently aim at the isotopes of hydrogen and helium: the precise extraction of their radii may provide a hint at the solution of the puzzle. We present the first *ab initio* calculation of nuclear structure corrections, including the nuclear polarization correction, to the 2S-2P transition in $\mu^3\text{He}^+$ and $\mu^3\text{H}$, and assess solid theoretical error bars. Our predictions reduce the uncertainty in the nuclear structure corrections to the level of a few percents and will be instrumental to the on-going $\mu^3\text{He}^+$ experiment. We also support the mirror $\mu^3\text{H}$ system as a candidate for further probing of the nucleon polarizabilities and shedding more light on the puzzle.

PACS numbers: 36.10.Ee, 21.60.De, 25.30.Mr, 31.30.jr, 21.10.Ft

I. INTRODUCTION

The root-mean-square (RMS) charge radius of the proton $r_p \equiv \sqrt{\langle r_p^2 \rangle}$ was recently determined with unprecedented precision from laser spectroscopy measurements of 2S-2P transitions in muonic hydrogen μH , where the electron is replaced by a muon [1, 2]. The extracted r_p differs by 7σ from the CODATA value [3], which is based in turn on many measurements involving electron-proton interactions. This discrepancy between the ‘muonic’ and ‘electronic’ proton radii ($r_p(\mu^-)$ and $r_p(e^-)$, respectively) is known as the “proton radius puzzle,” and has attracted much attention (see, *e.g.*, Ref. [4] for an extensive review and Ref. [5] for a brief summary of current results and ongoing experimental effort). In an attempt to solve the puzzle, extractions of $r_p(e^-)$ from the ample electron-proton (*ep*) scattering data have been reanalyzed by, *e.g.*, Refs. [6–9], while several planned experiments aim to re-measure *ep* scattering in new kinematic regions relevant for the puzzle [10, 11]. r_p extracted from electronic hydrogen is also being reexamined, both theoretically [12] and experimentally [13–15], as well as the Rydberg constant [15, 16], which is relevant for several radius extraction methods. A few of the theoretical attempts to account for the discrepancy between $r_p(e^-)$ and $r_p(\mu^-)$ include new interactions that violate lepton universality [17–19] and novel proton structures [20–24]. Yet the puzzle has not been solved. Answers may be provided

(see, *e.g.* Refs. [25, 26]) by a planned experiment at PSI [27] to scatter electrons, muons, and their antiparticles off the proton using the same experimental setup.

Alternatively, it will be insightful to study whether the puzzle also exists in other light nuclei, and whether it depends on the atomic mass A , charge number Z , or the number of neutrons N . In particular, the CREMA collaboration plans to extract high-precision charge radii from Lamb shift measurements that were recently performed in several hydrogen-like muonic systems [5, 28], namely, μD , $\mu^3\text{He}^+$, and $\mu^4\text{He}^+$. These measurements may unveil a dependence of the discrepancy on the isospin of the measured nucleus and, in particular, probe whether the neutron exhibits a similar effect as the puzzling proton. To obtain some control over these issues, it is advisable that nuclei with different N/Z ratios will be mapped out. It is the purpose of this Letter to perform an *ab initio* calculation of nuclear structure corrections (including nuclear polarization), with solid error estimates, for the $\mu^3\text{He}^+$ system and for its nuclear mirror, $\mu^3\text{H}$.

The Lamb shift [29] is the 2S-2P energy difference consisting of

$$\Delta E \equiv \delta_{\text{QED}} + \delta_{\text{FS}}(R_c) + \delta_{\text{TPE}}, \quad (1)$$

where, in decreasing order of magnitude, the three terms include: quantum electro-dynamics (QED) contributions from vacuum polarization, lepton self-energy, and relativistic recoil in δ_{QED} ; finite-nucleus-size contributions in $\delta_{\text{FS}}(R_c)$, where $R_c \equiv \sqrt{\langle R_c^2 \rangle}$ is the nuclear RMS charge radius; and contributions from two-photon exchange (TPE) between the lepton and the nucleus in δ_{TPE} . The last term can be divided into the elastic Zemach term and the inelastic polarization term, *i.e.*, $\delta_{\text{TPE}} = \delta_{\text{Zem}} + \delta_{\text{pol}}$. Additionally, each of these terms is separated into contributions from nuclear (δ^A) and nucleonic (δ^N) degrees

* nir.nevo@mail.huji.ac.il

† ji@ectstar.eu

‡ bacca@triumf.ca

§ nir@phys.huji.ac.il

of freedom, $\delta_{\text{TPE}} = \delta_{\text{Zem}}^A + \delta_{\text{Zem}}^N + \delta_{\text{pol}}^A + \delta_{\text{pol}}^N$.

In light muonic atoms, $\delta_{\text{QED}} \approx 10^2\text{--}10^3$ meV and is estimated from theory with a precision better than 10^{-3} meV [30–33]. At leading order $\delta_{\text{FS}}(R_c) = \frac{m_r^3(Z\alpha)^4}{12} R_c^2$, with m_r the reduced mass of the muon-nucleus system, while higher-order contributions are at the sub-percentage level [30]. The limiting factor for the attainable precision of R_c extracted from Eq. (1) is by far the uncertainty in δ_{TPE} . This was confirmed in two recent papers that reviewed the theory in μD [32], and in $\mu^4\text{He}$ and $\mu^3\text{He}$ [33]. Ref. [32] covers all the theoretical contributions to the Lamb shift in μD , including a summary of recent efforts by several groups [34–37] to accurately obtain δ_{TPE} in μD and reliably estimate its uncertainty, which comes out an order of magnitude larger than the uncertainties in the other terms. Ref. [33] details all the contributions for the two helium isotopes. Many terms are recalculated, not including the polarization correction δ_{pol} . For $\mu^4\text{He}^+$, *ab initio* nuclear calculations were recently applied in Ref. [38], improving on decades-old estimates of δ_{pol} . For three-body nuclei, the only calculations of δ_{pol} are outdated; based on old and simplistic nuclear models, their results are either inaccurate [39] or imprecise [40], reinforcing the need for modern, accurate, *ab initio* calculations for the three-body nuclei.

II. NUCLEAR STRUCTURE CONTRIBUTIONS

The nuclear Zemach term δ_{Zem}^A enters Eq. (1) as the elastic nuclear-structure contribution to δ_{TPE}^A ¹. This term is of order $(Z\alpha)^5$ and is defined as

$$\delta_{\text{Zem}}^A = -\frac{m_r^4(Z\alpha)^5}{24} \langle r^3 \rangle_{(2)}, \quad (2)$$

where $\langle r^3 \rangle_{(2)}$ is the 3rd nuclear Zemach moment². Friar & Payne showed [43] that the first-order corrections in δ_{pol}^A contain a part that cancels δ_{Zem}^A exactly. Calculation of this part can thus be avoided, as was done in Ref. [34], providing only the sum $\delta_{\text{TPE}}^A = \delta_{\text{pol}}^A + \delta_{\text{Zem}}^A$. However, following Refs. [35, 38, 44], we calculate explicitly all the parts of δ_{pol}^A , including the Zemach term, as detailed below. This is done in order to: (a) allow comparison with other values in the literature, and (b) provide theoretical support for the alternative way of extracting R_c from Eq. (1) where the Zemach term is phenomenologically parameterized as [30]

$$\delta_{\text{Zem}}^A = \mathcal{C} \times R_c^3. \quad (3)$$

¹ δ_{Zem}^A was derived by Friar [41] as the first-order $Z\alpha$ correction to $\delta_{\text{FS}}(R_c)$ and is called the ‘Friar’ term in Ref. [32].

² We refer only to charge-charge Zemach moments; for more details see, *e.g.*, Ref. [42].

As in Refs. [35, 38], the energy correction due to nuclear polarization is obtained as a sum of contributions

$$\delta_{\text{pol}}^A = \left[\delta_{D1}^{(0)} + \delta_L^{(0)} + \delta_T^{(0)} + \delta_C^{(0)} + \delta_M^{(0)} \right] + \left[\delta_{R3}^{(1)} + \delta_{Z3}^{(1)} \right] + \left[\delta_{R2}^{(2)} + \delta_Q^{(2)} + \delta_{D1D3}^{(2)} \right] + \left[\delta_{NS}^{(1)} + \delta_{NS}^{(2)} \right]. \quad (4)$$

Detailed formulas pertaining to most of the terms in Eq. (4) are found in [38] and are not repeated here. The largest contribution comes from the leading term, $\delta_{D1}^{(0)}$, related to the electric dipole. To this we add relativistic longitudinal and transverse corrections $\delta_L^{(0)}$ and $\delta_T^{(0)}$, respectively, as well as Coulomb distortion corrections $\delta_C^{(0)}$. Here we follow Ref. [35] and include in $\delta_C^{(0)}$ only the logarithmically enhanced term from the next order in $Z\alpha$. We generalize the treatment in Ref. [35] of the magnetic term $\delta_M^{(0)}$ by using the impulse approximation operator that includes the orbital angular momentum [45]. First-order corrections $\delta_{R3}^{(1)}$ and $\delta_{Z3}^{(1)}$ are related to a proton-proton correlation term and to the 3rd nuclear Zemach moment, respectively. Finally, at the next order we have the monopole $\delta_{R2}^{(2)}$, quadrupole $\delta_Q^{(2)}$, and interference $\delta_{D1D3}^{(2)}$ terms. All the above terms are calculated using point nucleons. Finite-nucleon-size (NS) corrections appear in Eq. (4) as $\delta_{NS}^{(1)} = \delta_{R1}^{(1)} + \delta_{Z1}^{(1)}$ and $\delta_{NS}^{(2)}$, which we elaborate on below.

III. NUCLEON-SIZE CORRECTIONS

The TPE in the point-nucleon limit is expressed as the interaction of photons with the structureless charged protons, while the neutrons are ignored. In this limit, the point-proton density operator is

$$\hat{\rho}_p(\mathbf{R}) \equiv \frac{1}{Z} \sum_{a=1}^A \delta(\mathbf{R} - \mathbf{R}_a) \frac{1 + \tau_a^3}{2}, \quad (5)$$

where τ_a^3 is the isospin projection operator. When the finite nucleon sizes are considered, $\hat{\rho}_p(\mathbf{R})$ must be convoluted with the proton’s internal charge distribution, and a similar convolution is applied to the point-neutron density operator

$$\hat{\rho}_n(\mathbf{R}) \equiv \frac{1}{N} \sum_{a=1}^A \delta(\mathbf{R} - \mathbf{R}_a) \frac{1 - \tau_a^3}{2}. \quad (6)$$

Following Refs. [38, 44], we apply a low-momentum expansion for the nucleon form factors, parameterized here by their mean square charge radii, $r_{n/p}^2 \equiv \langle r_{n/p}^2 \rangle$. We adopt $r_n^2 = -0.1161(22) \text{ fm}^2$ [46]. For the proton, we may use either $r_p(e^-) = 0.8775(51) \text{ fm}$ [3] or $r_p(\mu^-) = 0.84087(39) \text{ fm}$ [2]. In fact, until the ‘proton radius puzzle’ is resolved (or when R_c and other properties of the nuclei under consideration are measured using

muons), we should use $r_p(e^-)$ for comparison with the literature, which is based on data obtained with electrons, and $r_p(\mu^-)$ for predictions in muonic systems.

The leading NS correction $\delta_{NS}^{(1)}$ is the sum of nucleon-nucleon correlations in $\delta_{R1}^{(1)}$ and Zemach-like terms in $\delta_{Z1}^{(1)}$. The former is expressed as

$$\delta_{R1}^{(1)} = -\frac{m_r^4(Z\alpha)^5}{6} \iint d\mathbf{R}d\mathbf{R}' |\mathbf{R} - \mathbf{R}'| \left[r_p^2 \langle 0 | \hat{\rho}_p^\dagger(\mathbf{R}) \hat{\rho}_p(\mathbf{R}') | 0 \rangle \right. \\ \left. + \frac{N}{Z} r_n^2 \langle 0 | \hat{\rho}_n^\dagger(\mathbf{R}) \hat{\rho}_p(\mathbf{R}') | 0 \rangle \right], \quad (7)$$

which includes proton-proton (pp) and neutron-proton (np) correlations. It is an NS correction to the point-nucleon contribution $\delta_{R3}^{(1)}$ of Eq. (4) (the latter is denoted $\delta_{R3pp}^{(1)}$ in Ref. [38]). For the calculation of Zemach-like terms using point-nucleons we define

$$\langle r_{ij}^k \rangle_{(2)} \equiv \iint d\mathbf{R}d\mathbf{R}' |\mathbf{R} - \mathbf{R}'|^k \langle 0 | \hat{\rho}_i^\dagger(\mathbf{R}) | 0 \rangle \langle 0 | \hat{\rho}_j(\mathbf{R}') | 0 \rangle, \quad (8)$$

with i, j denoting either p or n . The 3rd nuclear Zemach moment is thus calculated as

$$\langle r^3 \rangle_{(2)} \approx \langle r_{pp}^3 \rangle_{(2)} + 4 \left[r_p^2 \langle r_{pp}^1 \rangle_{(2)} + \frac{N}{Z} r_n^2 \langle r_{np}^1 \rangle_{(2)} \right], \quad (9)$$

where the first term is the point-nucleon limit and the second is the (approximated) NS correction. Accordingly, the point-nucleon Zemach term $\delta_{Z3}^{(1)}$ and its NS correction $\delta_{Z1}^{(1)}$ are obtained by inserting Eq. (9) into Eq. (2) and flipping the sign, *i.e.*, $\delta_{Zem}^A \approx -(\delta_{Z3}^{(1)} + \delta_{Z1}^{(1)})$.

The sub-leading NS correction $\delta_{NS}^{(2)}$ is evaluated through a sum rule of the dipole response³

$$\delta_{NS}^{(2)} = -\frac{8\pi}{27} m_r^5 (Z\alpha)^5 \left[r_p^2 - \frac{N}{Z} r_n^2 \right] \int_{\omega_{th}}^{\infty} d\omega \sqrt{\frac{\omega}{2m_r}} S_{D1}(\omega). \quad (10)$$

Lastly, the nucleonic TPE correction δ_{TPE}^N also enters Eq. (1). We defer the treatment of this hadronic contribution to a dedicated section below.

IV. METHODS

Most of the above contributions can be written as sum rules of several nuclear responses with various energy-dependent weight functions [35, 38]. They were evaluated using the newly developed Lanczos sum rule method [47]. Ground-state observables of ^3He and ^3H , as well as Lanczos coefficients, were obtained using the effective interaction hyperspherical harmonics (EIHH) method [48, 49].

As only ingredients we employed in the nuclear Hamiltonian either one of the following state-of-the-art nuclear potentials: (i) the phenomenological AV18/UIX potential with two-nucleon [50] plus three-nucleon [51] forces; and (ii) the chiral effective field theory χEFT potential with two-nucleon [52] plus three-nucleon [53] forces.

It is of utmost importance to have realistic uncertainty estimates for our nuclear TPE predictions. These terms are the least well known in Eq. (1), and their uncertainties determine the attainable precision of R_c extracted from Lamb shift measurements. We considered many sources of uncertainty, namely: numerical; nuclear model; isospin symmetry breaking; higher-order nucleon-size corrections; missing relativistic and Coulomb-distortion corrections; higher multipoles, terms of higher-order in $Z\alpha$; and the effect of meson-exchange currents on the magnetic contribution. Their individual and cumulative effect on δ_{pol}^A , δ_{Zem}^A , and δ_{TPE}^A have been estimated and applied to the results given below. More details about these uncertainty estimates are given in the Supplementary Materials [54].

A. Results

We first compare a few observables we have calculated for the ^3He and ^3H nuclei with corresponding theoretical and experimental values available in the literature. In Table I we present the ground-state binding energy BE, charge radius R_c , and magnetic moment $\hat{\mu}_{gs}$, as well as the electric dipole polarizability α_E . In general, good agreement is found with other calculations.

Our results do not include isospin-symmetry breaking (ISB), except for the Coulomb interaction between protons in ^3He . Calculations by other groups shown in Table I usually do not include ISB effects; notable exceptions are Ref. [56], which includes the $T = 3/2$ isospin channel in the ground-state wave function, and Ref. [55] that provides results either including or excluding it. One observes that including ISB alters BE by a few keV. In addition, the ^3He BE, not used in the calibration of the Hamiltonians, is overestimated at a sub-percentage level, and this is slightly *worsened* when ISB is included. As discussed in Ref. [62], changes in BE shift the threshold of sum rules, affecting mostly sum rules with inverse energy dependence, such as α_E discussed below. For the other observables in Table I, the estimated uncertainty stemming from ISB is $\lesssim 1\%$.

Charge radii R_c shown in Table I are obtained from the calculated point-proton-distribution RMS radius R_p as [66, 67]

$$R_c^2 = R_p^2 + r_p^2 + \frac{N}{Z} r_n^2 + \frac{3}{4m_p^2}, \quad (11)$$

where we omit contributions from the spin-orbit radius (negligible for s-shell nuclei) and meson-exchange currents. The last term in Eq. (11) is the Darwin-Foldy term, where m_p is the proton mass, taken from

³ The sign before r_n^2 in Eq. (10) is corrected from Refs. [35, 38] and agrees with Ref. [37].

Table I. Various ${}^3\text{He}$ and ${}^3\text{H}$ observables (see text for details) calculated with the AV18/UIX and χEFT potentials, compared to corresponding calculations in the literature and to experimental values. Our ground-state wave functions do not include the $T = 3/2$ channel. Our numerical uncertainties are not shown since they are smaller than one in the last decimal place. References labels correspond to: ^{a/b} Ref. [55] without/with inclusion of the $T = 3/2$ channel, respectively; ^c Ref. [56] (which includes the $T = 3/2$ channel); ^d Ref. [57]; ^e Ref. [58]; ^f Ref. [59]; ^g Ref. [60]; ^h Ref. [61]; ⁱ Ref. [62]; ^j Ref. [40]; ^k Ref. [63]; ^l Ref. [64]; ^m Ref. [65].

${}^3\text{He}$	BE [MeV]	$R_c(e^-)$ [fm]	$\hat{\mu}_{gs}$ [μ_N]	α_E [fm^3]
AV18/UIX	7.740	1.968	-1.73	0.149
Lit.	7.740(1) ^a	-	-1.764 ^e	0.153(15) ^g
	7.748(1) ^b	-	-1.749 ^f	0.145 ^h
χEFT	7.735	1.988	-1.76	0.153
Lit.	7.750 ^c	-	-	0.149(5) ⁱ
Exp.	7.71804 ^d	1.966(3) ^m	-2.127 ^d	0.130(13) ^j 0.250(40) ^k
${}^3\text{H}$	BE [MeV]	$R_c(e^-)$ [fm]	$\hat{\mu}_{gs}$ [μ_N]	α_E [fm^3]
AV18/UIX	8.473	1.755	2.59	0.137
Lit.	8.472(1) ^a	-	2.575 ^e	0.139(4) ^l
	8.478(1) ^b	-	2.569 ^f	
χEFT	8.478	1.777	2.63	0.139
Lit.	8.474 ^c	-	-	0.139(2) ⁱ
Exp.	8.48180 ^d	1.759(36) ^m	2.979 ^d	

Refs. [3, 46]. In Table I, we show only R_c values obtained using $r_p(e^-)$ and experimental values obtained only with electrons. As a direct result of Eq. (11), using $r_p(\mu^-)$ would decrease R_c by 0.016 (0.018) fm for ${}^3\text{He}$ (${}^3\text{H}$). We note that the uncertainty, currently governed by nuclear-model dependence, is slightly larger than the effect of varying r_p . It should also be noted that our R_p values agree with the hyperspherical harmonics calculations of the Pisa group [56] for both nuclear potentials, suggesting a small ISB effect, while the Monte-Carlo calculations of Ref. [59] show less agreement and hint at a larger ISB effect. Considering that radii were not included in the calibration of the nuclear Hamiltonians, it would be interesting to further investigate their sensitivity to the theoretical apparatus. In particular, work is in progress to include meson-exchange currents [68]. Currently, for ${}^3\text{He}$ the AV18/UIX charge radius is in better agreement with the experimental value, while for ${}^3\text{H}$ the experimental error bar is larger than the nuclear-model dependence, and calls for a more precise measurement.

Concerning the magnetic moments, our results are comparable with the other impulse approximation calculations presented in Table I, which deviate from experiment due to the absence of meson-exchange currents. However, we do not include meson-exchange currents in δ_{TPE}^A , since the contribution of the magnetic term $\delta_M^{(0)}$ is small enough to make these corrections negligible.

The electric dipole polarizability α_E is an inverse-energy-weighted sum rule of the dipole response and is therefore closely related to δ_{pol}^A . Our results are in agreement with previous calculations, especially the recent Ref. [62]. As in [38], α_E is found to be nuclear-model dependent. We provide first results for the unmeasured α_E of ${}^3\text{H}$ with the AV18/UIX potential, which lies within the uncertainty estimates of [62].

We now turn to the Zemach terms, first listing available values in the literature. In Refs. [30, 31] Borie calculated δ_{Zem}^A , following Friar [41], using a Gaussian distribution that fits the nuclear-charge-radius obtained from electron experiments. The result^{4,5} was $\delta_{\text{Zem}}^A({}^3\text{He}) = -10.258(305)$ meV. Recently, Krutov et al. [33] repeated this calculation and obtained $\delta_{\text{Zem}}^A({}^3\text{He}) = -10.28(10)$ meV. Alternatively, inserting the 3rd nuclear Zemach moment recently extracted from $e-{}^3\text{He}$ scattering data [69] into Eq. (2) gives $\delta_{\text{Zem}}^A({}^3\text{He}) = -10.87(27)$ meV. As explained above, all of these results should be compared with our calculation that uses $r_p(e^-)$ as input and yields $\delta_{\text{Zem}}^A({}^3\text{He})[r_p(e^-)] = -10.71(19)(16)$ meV, where the first uncertainty results from nuclear-model dependence and the second includes all other sources. Our result is in agreement with these references (based on comments made in Refs. [33, 69], we assume that the error-bars in Ref. [33] are not exhaustive). However, for the muonic systems considered here we use $r_p(\mu^-)$, which gives

$$\delta_{\text{Zem}}^A({}^3\text{He})[r_p(\mu^-)] = -10.49(19)(16) \text{ meV}. \quad (12)$$

We note that with the given error-bars this result is also in agreement with Refs. [31, 33, 69].

The use of Eq. (3) is adopted from Refs. [30, 31], where⁶ $\mathcal{C}({}^3\text{He}) = -1.35(4)$ meV fm⁻³. The results of Ref. [69] can also be used to extract $\mathcal{C}({}^3\text{He}) = \delta_{\text{Zem}}^A/R_c^3 = -1.42(4)$ meV fm⁻³ from the $e-{}^3\text{He}$ scattering data. Our calculations of δ_{Zem}^A and R_c with either value of r_p give $\mathcal{C}({}^3\text{He})[r_p(e^-)] = -1.383(05)(20)$ meV fm⁻³ and $\mathcal{C}({}^3\text{He})[r_p(\mu^-)] = -1.388(05)(21)$ meV fm⁻³, which both agree with Refs. [30, 31, 69]. Evidently, the nuclear-model dependence is diminished for this value, since it is proportional to the geometrical ratio $\langle r^3 \rangle_{(2)}/R_c^3$. Similarly to R_c discussed above, the difference between δ_{Zem}^A results obtained with the two nuclear potentials stems from the different point-proton distributions, and this largely cancels out in \mathcal{C} , reducing its total relative uncertainty compared to δ_{Zem}^A .

Repeating the above procedures we obtain predictions for $\mu^3\text{H}$

$$\delta_{\text{Zem}}^A({}^3\text{H})[r_p(\mu^-)] = -0.227(5)(3) \text{ meV}, \quad (13)$$

⁴ Ref. [31] is the arXiv version of Ref. [30], which has been updated since publication; in particular, $\delta_{\text{Zem}}^A({}^3\text{He})$ was increased by $\sim 20\%$ with respect to the published version.

⁵ The result is given using our sign convention.

⁶ See footnote 5.

and

$$\mathcal{C}({}^3\text{H})[r_p(\mu^-)] = -0.0425(2)(6) \text{ meV fm}^{-3}. \quad (14)$$

For future comparisons, using $r_p(e^-)$ shifts $\delta_{\text{Zem}}^A({}^3\text{H})$ by $-6 \text{ } \mu\text{eV}$ and $\mathcal{C}({}^3\text{H})$ by $+0.2 \text{ } \mu\text{eV fm}^{-3}$.

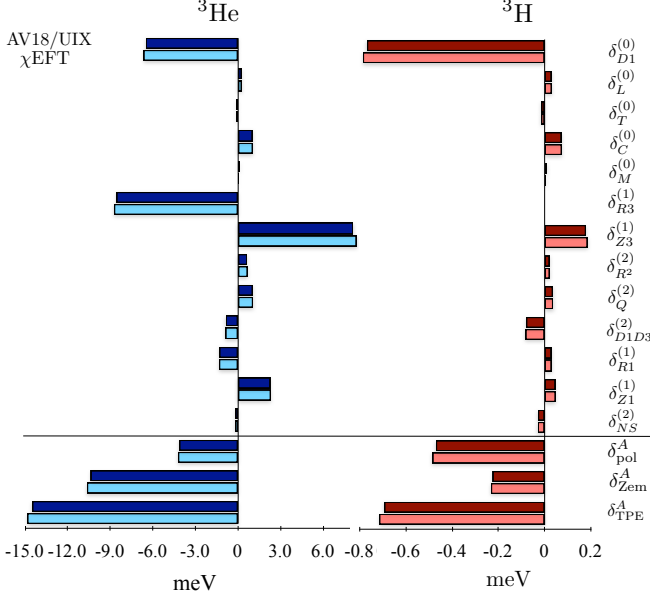


Figure 1. Graphic representation of the various contributions to the nuclear structure and polarization corrections to the 2S-2P Lamb shift in the muonic hydrogen-like systems of ${}^3\text{He}$ and ${}^3\text{H}$, calculated with the AV18/UIX and χEFT nuclear potentials. Notice the different scales used for the two systems.

Next, the nuclear polarization correction to the Lamb shift — δ_{pol}^A — is obtained by summing up the terms in Eq. (4). Their values for $\mu^3\text{He}^+$ and $\mu^3\text{H}$, calculated with the two nuclear potentials, are shown⁷ in Fig. 1. Here, the NS corrections are obtained using only $r_p(\mu^-)$. Taking the mean value of the two nuclear potentials we obtain

$$\begin{aligned} \delta_{\text{pol}}^A(\mu^3\text{He}^+) &= -4.16(06)(16) \text{ meV} \\ \delta_{\text{pol}}^A(\mu^3\text{H}) &= -0.476(10)(13) \text{ meV}, \end{aligned} \quad (15)$$

where we retain the use of first and second brackets for uncertainties from nuclear-model dependence and from all other sources, respectively. Our result for $\mu^3\text{He}^+$ agrees with Rinker's $-4.9 \pm 1.0 \text{ meV}$ obtained forty years ago [40]. The $\mu^3\text{H}$ case was rarely studied. We note, however, that a comparison with the simplistic calculation of Ref. [39] reveals a similar ratio of ~ 9 between δ_{pol}^A of $\mu^3\text{He}^+$ and of $\mu^3\text{H}$, both in Ref. [39] and in our work.

⁷ The numerical values are detailed in the Supplementary Materials [54].

Adding Eqs. (12) and (13) to Eq. (15) we obtain the total nuclear-structure TPE corrections that enter Eq. (1)

$$\begin{aligned} \delta_{\text{TPE}}^A(\mu^3\text{He}^+) &= -14.64(25)(27) \text{ meV} \\ \delta_{\text{TPE}}^A(\mu^3\text{H}) &= -0.703(16)(11) \text{ meV}. \end{aligned} \quad (16)$$

V. HADRONIC TPE

The last ingredient in δ_{TPE} is the contribution from two-photon exchange with the internal degrees of freedom of the nucleons that make up the nucleus, *i.e.*, $\delta_{\text{TPE}}^N = \delta_{\text{Zem}}^N + \delta_{\text{pol}}^N$. Since it is dictated by the hadronic scale, about 10 times higher than the nuclear interaction, this contribution can be approximated as the sum of TPE effects with each of the individual nucleons. The various terms that contribute to δ_{TPE}^N are estimated based on previous studies of μH , as recently done for μD in Ref. [32]. Specifically, as suggested by Birse and McGovern [70], we adopt values of δ_{Zem} and δ_{pol} in μH that are combinations of results from Refs. [21, 71], as detailed below.

As Friar showed in Ref. [72], the intrinsic Zemach term of each proton contributes to δ_{TPE} of the nucleus as an additional NS correction, not accounted for in the NS corrections detailed above⁸. We denote this term δ_{Zem}^N and find its contribution to be proportional to the analogous term in μH by

$$\delta_{\text{Zem}}^N(\mu\text{A}) = \left(\frac{Zm_r(\mu\text{A})}{m_r(\mu\text{H})} \right)^4 \times \delta_{\text{Zem}}(\mu\text{H}). \quad (17)$$

We take $\delta_{\text{Zem}}(\mu\text{H}) = 0.0247(13) \text{ meV}$ ⁹ and obtain

$$\begin{aligned} \delta_{\text{Zem}}^N(\mu^3\text{He}^+) &= -0.487(26) \text{ meV} \\ \delta_{\text{Zem}}^N(\mu^3\text{H}) &= -0.0305(16) \text{ meV}. \end{aligned} \quad (18)$$

In Ref. [36], δ_{pol}^N of μD was extracted from electron scattering data. Here, we resort to estimating δ_{pol}^N by relating it to the proton polarization correction in μH via [34, 37, 75]

$$\delta_{\text{pol}}^N(\mu\text{A}) = (N + Z) [Zm_r(\mu\text{A})/m_r(\mu\text{H})]^3 \delta_{\text{pol}}(\mu\text{H}), \quad (19)$$

assuming that the neutron polarization contribution is the same as that of the proton. Here we use $\delta_{\text{pol}}(\mu\text{H}) = 9.3(1.1) \text{ } \mu\text{eV}$ ¹⁰. Based on current knowledge of the nucleon polarizabilities [76], we assign an additional

⁸ In our notations this term appears as an NS correction to $\delta_{R3}^{(1)}$.
⁹ We use the same value as in [32]. Here, $\delta_{\text{Zem}}(\mu\text{H})$ stands for the elastic + non-pole parts of $\delta_{\text{TPE}}(\mu\text{H})$, and not for the non-relativistic limit that is related to the proton's 3rd Zemach moment (see Refs. [73, 74]).

¹⁰ $\delta_{\text{pol}}(\mu\text{H}) = \delta_{\text{inelastic}}^p + \delta_{\text{subtraction}}^p$. For the former we follow Ref. [36] and adopt $13.5 \text{ } \mu\text{eV}$, which is an average of three values from Ref. [71], and for the latter we use $-4.2(1.0) \text{ } \mu\text{eV}$ from Ref [21].

20% uncertainty to the neutron polarization contribution. Another possible error in δ_{pol}^N arises from neglecting medium effects and nucleon-nucleon interferences in Eq. (19). These effects can be estimated by comparing the calculated $\delta_{\text{pol}}^N(\mu\text{D})$ with the result evaluated in Ref. [36] from scattering data. This yields a $\sim 29\%$ correction. Until this correction is calculated rigorously in other light muonic atoms, we estimate it to be of a similar size, multiplied by $A/2$, making it the dominant source of uncertainty in our δ_{TPE}^N . Eventually, we obtain

$$\begin{aligned}\delta_{\text{pol}}^N(\mu^3\text{He}^+) &= -0.275(123) \text{ meV} \\ \delta_{\text{pol}}^N(\mu^3\text{H}) &= -0.034(16) \text{ meV} .\end{aligned}\quad (20)$$

Summing up the results in Eqs. (18) and (20) we obtain the total contribution from the nucleon degrees of freedom

$$\begin{aligned}\delta_{\text{TPE}}^N(\mu^3\text{He}^+) &= -0.762(125) \text{ meV} \\ \delta_{\text{TPE}}^N(\mu^3\text{H}) &= -0.065(16) \text{ meV} .\end{aligned}\quad (21)$$

In $\mu^3\text{He}^+$, δ_{TPE}^N is $\sim 5\%$ of δ_{TPE}^A , *i.e.*, about twice the overall uncertainty in δ_{TPE}^A . For $\mu^3\text{H}$ we obtained that δ_{TPE}^N is $\sim 9\%$ of δ_{TPE}^A , which is more than three times the uncertainty in the latter. Therefore, our precision in predicting δ_{TPE}^A can be important not only for the determination of R_c from muonic Lamb shift measurements, but also for probing δ_{TPE}^N , if these measurements reveal discrepancies with electronic experiments that may indicate exotic contributions to δ_{TPE}^N . A study of the Lamb shift in $\mu^3\text{H}$ will be especially sensitive to the nucleon polarizabilities, since their relative contribution is much larger in this case.

VI. SUMMARY

We have performed the first *ab initio* calculation of δ_{Zem}^A and δ_{pol}^A for both $\mu^3\text{He}^+$ and $\mu^3\text{H}$, using state-

of-the-art nuclear potentials. Many possible sources of uncertainty have been considered, yet the resulting uncertainties of a few percents are much lower than in previous estimates of δ_{pol}^A and δ_{TPE}^A , which relied on imprecise data and simplistic models. In addition, our δ_{Zem}^A calculations agree with previous estimates and with recent analysis of $e^-^3\text{He}$ scattering, and provide predictions towards ^3H measurements. They were also adapted for muonic systems by incorporating $r_p(\mu^-)$ — the proton radius measured with muons.

Ultimately, our results will allow two alternative ways of extracting a much more precise R_c from a recent measurement [5, 28, 77] of the Lamb shift in $\mu^3\text{He}^+$, and from an analogous measurement we encourage to conduct in $\mu^3\text{H}$. The precision of the charge radii of ^3He and ^3H could be thus improved by factors of ~ 5 and ~ 50 , respectively, which could have interesting implications for nuclear physics.

Finally, we estimate the hadronic contribution δ_{TPE}^N in these systems, and find it to be larger than our uncertainty estimates in δ_{TPE}^A . Therefore, this combined theoretical and experimental effort may not only shed some light on the “proton radius puzzle,” but could also probe the elusive nucleon polarizabilities tightly connected to it.

ACKNOWLEDGMENTS

NND would like to thank Bezalel Bazak for suggesting the case of muonic triton, to express a special thanks to the Mainz Institute for Theoretical Physics (MITP) for its hospitality and support, and acknowledge constructive discussions with Aldo Antognini, Mike Birse, Michael Distler, Mikhail Gorchtein, Savely Karshenboim, Franz Kottmann, Randolph Pohl, and Ingo Sick. This work was supported in parts by the Natural Sciences and Engineering Research Council (NSERC), the National Research Council of Canada, the Israel Science Foundation (Grant number 954/09), and the Pazy foundation.

-
- [1] R. Pohl *et al.*, *Nature* **466**, 213 (2010).
 - [2] A. Antognini *et al.*, *Science* **339**, 417 (2013).
 - [3] P. J. Mohr, B. N. Taylor, and D. B. Newell, *Rev. Mod. Phys.* **84**, 1527 (2012).
 - [4] R. Pohl, R. Gilman, G. A. Miller, and K. Pachucki, *Ann. Rev. of Nucl. and Part. Sci.* **63**, 175 (2013).
 - [5] R. Pohl, *Hyperfine Interactions* **227**, 23 (2014).
 - [6] R. J. Hill and G. Paz, *Phys. Rev. D* **82**, 113005 (2010).
 - [7] I. Sick and D. Trautmann, *Phys. Rev. C* **89**, 012201 (2014).
 - [8] E. Kraus, K. Mesick, A. White, R. Gilman, and S. Strauch, *Phys. Rev. C* **90**, 045206 (2014), [arXiv:1405.4735 \[nucl-ex\]](#).
 - [9] I. Lorenz, U.-G. Meißner, H.-W. Hammer, and Y.-B. Dong, *Phys. Rev. D* **91**, 014023 (2015).
 - [10] A. Gasparin *et al.*, “High precision measurement of the proton charge radius,” Jefferson Laboratory Experiment 12-11-106 (unpublished) (2012).
 - [11] M. Mihovilovic, H. Merkel, and A1-Collaboration, *AIP Conf. Proc.* **1563**, 187 (2013).
 - [12] S. G. Karshenboim, *Phys. Rev. A* **91**, 012515 (2015).
 - [13] A. Vutha, N. Bezginov, I. Ferchichi, M. George, V. Isaac, C. Storry, A. Weatherbee, M. Weel, and E. Hessels, *Bulletin of the American Physical Society*, **57**, D1.00138 (2012).
 - [14] A. Beyer, J. Alnis, K. Khabarova, A. Matveev, C. G. Parthey, D. C. Yost, R. Pohl, T. Udem, T. W. Haensch, and N. Kolachevsky, *Annalen der Physik* **525**, 671 (2013).
 - [15] E. Peters, D. C. Yost, A. Matveev, T. W. Hensch, and T. Udem, *Annalen der Physik* **525**, L29 (2013).

- [16] J. N. Tan, S. M. Brewer, and N. D. Guise, *Physica Scripta* **2011**, 014009 (2011).
- [17] B. Batell, D. McKeen, and M. Pospelov, *Phys. Rev. Lett.* **107**, 011803 (2011).
- [18] D. Tucker-Smith and I. Yavin, *Phys. Rev. D* **83**, 101702 (2011).
- [19] C. E. Carlson and B. C. Rislow, *Phys. Rev. D* **89**, 035003 (2014).
- [20] R. J. Hill and G. Paz, *Phys. Rev. Lett.* **107**, 160402 (2011).
- [21] M. C. Birse and J. A. McGovern, *The European Physical Journal A* **48**, 120 (2012).
- [22] G. A. Miller, *Physics Letters B* **718**, 1078 (2013).
- [23] U. D. Jentschura, *Phys. Rev. A* **88**, 062514 (2013).
- [24] F. Hagelstein and V. Pascalutsa, *Phys. Rev. A* **91**, 040502 (2015).
- [25] G. A. Miller, A. W. Thomas, J. D. Carroll, and J. Rafelski, *Phys. Rev. A* **84**, 020101 (2011).
- [26] O. Tomalak and M. Vanderhaeghen, *Phys. Rev. D* **90**, 013006 (2014).
- [27] R. Gilman, *AIP Conference Proceedings* **1563**, 167 (2013).
- [28] A. Antognini *et al.*, *Can. J. of Phys.* **89**, 47 (2011).
- [29] W. E. Lamb and R. C. Retherford, *Phys. Rev.* **72**, 241 (1947).
- [30] E. Borie, *Annals of Physics* **327**, 733 (2012).
- [31] E. Borie, [arXiv:1103.1772 \[physics.atom-ph\]](#) (2014).
- [32] J. J. Krauth, M. Diepold, B. Franke, A. Antognini, F. Kottmann, and R. Pohl, [arXiv:1506.01298 \[physics.atom-ph\]](#) (2015).
- [33] A. Krutov, A. Martynenko, G. Martynenko, and R. Faustov, *Journal of Experimental and Theoretical Physics* **120**, 73 (2015).
- [34] K. Pachucki, *Phys. Rev. Lett.* **106**, 193007 (2011).
- [35] O. J. Hernandez, C. Ji, S. Bacca, N. Nevo Dinur, and N. Barnea, *Physics Letters B* **736**, 344 (2014).
- [36] C. E. Carlson, M. Gorchtein, and M. Vanderhaeghen, *Phys. Rev. A* **89**, 022504 (2014).
- [37] K. Pachucki and A. Wienczek, *Phys. Rev. A* **91**, 040503 (2015).
- [38] C. Ji, N. Nevo Dinur, S. Bacca, and N. Barnea, *Phys. Rev. Lett.* **111**, 143402 (2013).
- [39] C. Joachain, *Nuclear Physics* **25**, 317 (1961).
- [40] G. A. Rinker, *Phys. Rev. A* **14**, 18 (1976).
- [41] J. L. Friar, *Ann. of Phys.* **122**, 151 (1979).
- [42] M. O. Distler, J. C. Bernauer, and T. Walcher, *Physics Letters B* **696**, 343 (2011).
- [43] J. L. Friar and G. L. Payne, *Phys. Rev. A* **56**, 5173 (1997).
- [44] C. Ji, N. Nevo Dinur, S. Bacca, and N. Barnea, *Few-Body Systems* **55**, 917 (2014).
- [45] P. Ring and P. Schuck, *The nuclear many-body problem* (Springer-Verlag Berlin Heidelberg, 1980).
- [46] J. Beringer *et al.* (Particle Data Group), *Phys. Rev. D* **86**, 010001 (2012).
- [47] N. Nevo Dinur, N. Barnea, C. Ji, and S. Bacca, *Phys. Rev. C* **89**, 064317 (2014).
- [48] N. Barnea, W. Leidemann, and G. Orlandini, *Phys. Rev. C* **61**, 054001 (2000).
- [49] N. Barnea, W. Leidemann, and G. Orlandini, *Nuclear Physics A* **693**, 565 (2001).
- [50] R. B. Wiringa, V. G. J. Stoks, and R. Schiavilla, *Phys. Rev. C* **51**, 38 (1995).
- [51] B. S. Pudliner, V. R. Pandharipande, J. Carlson, and R. B. Wiringa, *Phys. Rev. Lett.* **74**, 4396 (1995).
- [52] D. R. Entem and R. Machleidt, *Phys. Rev. C* **68**, 041001 (2003).
- [53] P. Navrátil, *Few-Body Systems* **41**, 117 (2007).
- [54] Additional details are available as supplementary materials online.
- [55] A. Nogga, A. Kievsky, H. Kamada, W. Glöckle, L. E. Marcucci, S. Rosati, and M. Viviani, *Phys. Rev. C* **67**, 034004 (2003).
- [56] A. Kievsky, S. Rosati, M. Viviani, L. E. Marcucci, and L. Girlanda, *Journal of Physics G: Nuclear and Particle Physics* **35**, 063101 (2008).
- [57] J. Purcell, J. Kelley, E. Kwan, C. Sheu, and H. Weller, *Nuclear Physics A* **848**, 1 (2010).
- [58] L. E. Marcucci, M. Pervin, S. C. Pieper, R. Schiavilla, and R. B. Wiringa, *Phys. Rev. C* **78**, 065501 (2008).
- [59] S. Pastore, S. C. Pieper, R. Schiavilla, and R. B. Wiringa, *Phys. Rev. C* **87**, 035503 (2013).
- [60] K. Pachucki and A. M. Moro, *Phys. Rev. A* **75**, 032521 (2007).
- [61] W. Leidemann, in *Few-Body Problems in Physics '02*, Few-Body Systems, Vol. 14, edited by R. Krivec, M. Rosina, B. Golli, and S. irca (Springer Vienna, 2003) pp. 313–318.
- [62] I. Stetcu, S. Quaglioni, J. L. Friar, A. C. Hayes, and P. Navrátil, *Phys. Rev. C* **79**, 064001 (2009).
- [63] F. Goeckner, L. O. Lamm, and L. D. Knutson, *Phys. Rev. C* **43**, 66 (1991).
- [64] V. D. Efros, W. Leidemann, and G. Orlandini, *Physics Letters B* **408**, 1 (1997).
- [65] I. Angeli and K. P. Marinova, *Atomic Data and Nuclear Data Tables* **99**, 69 (2013).
- [66] J. L. Friar, J. Martorell, and D. W. L. Sprung, *Phys. Rev. A* **56**, 4579 (1997).
- [67] A. Ong, J. C. Berengut, and V. V. Flambaum, *Phys. Rev. C* **82**, 014320 (2010).
- [68] S. Pastore, C. Ji, N. Nevo Dinur, S. Bacca, M. Piarulli, R. B. Wiringa, and N. Barnea, in preparation.
- [69] I. Sick, *Phys. Rev. C* **90**, 064002 (2014).
- [70] M. C. Birse and J. A. McGovern, private communication (2015).
- [71] C. E. Carlson and M. Vanderhaeghen, *Phys. Rev. A* **84**, 020102 (2011).
- [72] J. L. Friar, *Phys. Rev. C* **88**, 034003 (2013).
- [73] A. Antognini *et al.*, *Science* **339**, 417 (2013), supplementary materials.
- [74] A. Antognini, F. Kottmann, F. Biraben, P. Indelicato, F. Nez, and R. Pohl, *Annals of Physics* **331**, 127 (2013).
- [75] G. A. Miller, [arXiv:1501.01036 \[nucl-th\]](#) (2015).
- [76] L. S. Myers, J. R. M. Annand, J. Brudvik, G. Feldman, K. G. Fissum, H. W. Griebhammer, K. Hansen, S. S. Henshaw, L. Isaksson, R. Jebali, M. A. Kovash, M. Lundin, J. A. McGovern, D. G. Middleton, A. M. Nathan, D. R. Phillips, B. Schröder, and S. C. Stave ((COMPTON@MAX-lab Collaboration)), *Phys. Rev. Lett.* **113**, 262506 (2014).
- [77] F. Kottmann, private communication (2014).

Supplementary Materials

Appendix A: error estimation

We consider many sources of uncertainty. Below we explain the origin and derivation of each uncertainty estimate.

Numerical: First we estimate the numerical accuracy of the calculations. In the EIHH method [48, 49], the calculations are usually repeated with the model space truncated at increasing values of the maximal hyperangular momentum K_{\max} , until the differences between consecutive K_{\max} results become negligible. Accordingly, the numerical uncertainty can be estimated, as in [38], from the difference between two results obtained with different K_{\max} values. However, unlike Ref. [38], here we encountered very slow convergence¹¹, especially with the χ EFT potential, and particularly for the $\delta^{(2)}$ terms, which turned out to be more sensitive to the parameterization of the hyperradial grid. Consequently, the final values we provide for many terms¹² were obtained by extrapolating the results of several calculations made with different K_{\max} values. Therefore, for some of our results the numerical uncertainty was estimated from these extrapolations.

Nuclear model: Next we note the dependence of the results on the nuclear model, which is probed as in Ref. [38] by using the AV18/UIX and χ EFT potentials. The final values we present are obtained by taking the mean value of the two results. As in Refs. [35, 38], the corresponding uncertainty is estimated as their difference divided by $\sqrt{2}$, to account for the possibility that the “true” result lies outside the range bounded by the two calculated results.

ISB: The next source of uncertainty stems from the conservation of isospin symmetry in our calculations, *i.e.*, we assume that the total isospin is a conserved quantity throughout the calculation. All nucleons are taken to be of equal mass, which is the average between the proton and neutron masses. The difference between the proton and the neutron is manifested only in their gyromagnetic factors and in the electromagnetic interaction included in the NN interaction. In the $A = 3$ nuclei, most of the isospin symmetry breaking (ISB) effect can be accounted for by allowing the nuclear ground-state wave functions to include also the channel with higher total isospin value $T = 3/2$. This, however, increases the number of basis states in each calculation and the associated computational cost rises rapidly with K_{\max} . It was therefore performed selectively only to estimate the uncertainty associated with performing isospin conserving calculations.

Nucleon-size corrections: Comparing the coordinate-space and momentum-space treatments of the NS corrections we conclude that higher-order corrections to the terms we obtained are expected only at $\delta_{NS}^{(1)}$. For the Zemach moments we were able to undertake a more accurate approach, from which we estimate these higher-order corrections to be $\sim 1.46\%$ ($\sim 1.33\%$) for $\mu^3\text{He}^+$ ($\mu^3\text{H}$). However, for consistency we use here only the low- Q^2 approximation of the nucleon electric form factor, and use the above corrections to estimate the NS-related uncertainties of the $\delta^{(1)}$ terms.

Relativistic corrections: As explained in Section 2, relativistic corrections were included only for the leading electric dipole contribution $\delta_{D1}^{(0)}$. Their sum turned out to be 2.0% (2.1%) of the non-relativistic value in ^3He (^3H). We therefore estimated the uncertainty due to uncalculated relativistic corrections of the other contributions to be of that relative size. We would like to point out two aspects of the elastic (Zemach) term: (i) Comparing the non-relativistic calculation of δ_{Zem}^A of μD in Ref. [35] with the relativistic treatment in Ref. [36] reveals a discrepancy of the same order as the uncertainty estimate given above. (ii) We calculate δ_{Zem}^A according to the definition that connects it to the nuclear Zemach moments. Therefore, no relativistic corrections are needed in the comparison we make with similar results in the literature. However, when our value for \mathcal{C} is used to approximate the full elastic part of δ_{TPE}^A in Eq. (1), the missing relativistic corrections should be accounted for. In this context, the total relative uncertainty of \mathcal{C} should be increased to 2.5%.

Coulomb corrections: Following Ref. [37], we estimate higher-order Coulomb corrections to be $\sim 6\%$ of $\delta^{(2)}$.

Multipole expansion: As in Ref. [38], our multipole expansion is truncated at $\delta^{(2)}$. Based on our results we conservatively estimate 2% uncertainty in δ_{pol}^A due to this truncation.

¹¹ This may be due to the larger radii of the $A = 3$ nuclei compared with ^4He , and was indeed slightly worse for ^3He than for ^3H .

¹² Depending on the nucleus and the nuclear potential, some of the

following terms were obtained with the aid of extrapolations: BE, α_E , the individual $\delta^{(2)}$ terms (including $\delta_{NS}^{(2)}$, $\delta_M^{(0)}$, and the sum of all other $\delta^{(0)}$ terms.

$Z\alpha$ expansion: Except for the logarithmically enhanced Coulomb distortion contribution, we include in our calculation of δ_{pol}^A all terms of order $(Z\alpha)^5$. Since $(Z\alpha)$ is small for these systems, the missing contribution from all the higher-order terms can be approximated by the first unaccounted-for term in the series, $(Z\alpha)^6$, which is naturally estimated to be $(Z\alpha) \simeq 1.46\%$ (0.73%) of the size of δ_{pol}^A in ${}^3\text{He}$ (${}^3\text{H}$).

Magnetic MEC contribution: The magnetic dipole term $\delta_M^{(0)}$ is calculated using the impulse approximation (IA) operator, and is therefore missing significant corrections, mainly due to meson-exchange currents (MECs)¹³. The same IA operator was also used to calculate the magnetic moment $\hat{\mu}_{gs}$ in the nuclear ground state. The results, presented in Table I, show a deviation of the IA $\hat{\mu}_{gs}$ calculated with the AV18/UIX (χEFT) potential from the very precise experimental values by 23% (21%) for ${}^3\text{He}$ and 15% (13%) for ${}^3\text{H}$. The same relative errors were therefore assumed also for the small IA value obtained for $\delta_M^{(0)}$.

The total uncertainties were obtained as a quadrature sum of all the above, where the last five sources do not affect the Zemach terms. The values we thus obtained for the individual and total relative uncertainties estimated for δ_{pol}^A , δ_{Zem}^A , and δ_{TPE}^A in $\mu {}^3\text{He}^+$ and $\mu {}^3\text{H}$ are given in Table S1 below. We remind the reader that $\delta_{\text{TPE}}^A \equiv \delta_{\text{Zem}}^A + \delta_{\text{pol}}^A$ can be obtained directly from our results, by summing all terms in δ_{pol}^A except for the Zemach terms, due to their cancellation.

Table S1. Estimated relative uncertainties, in percents, assigned to the calculated nuclear TPE corrections to the 2S-2P Lamb shift in $\mu {}^3\text{He}^+$ and $\mu {}^3\text{H}$. The presented values are rounded. The total uncertainties are obtained from a quadrature sum.

Error type	$\mu {}^3\text{He}^+$			$\mu {}^3\text{H}$		
	δ_{pol}^A	δ_{Zem}^A	δ_{TPE}^A	δ_{pol}^A	δ_{Zem}^A	δ_{TPE}^A
Numerical	0.4	0.1	0.1	0.1	0.0	0.1
Nuclear model	1.5	1.8	1.7	2.2	2.3	2.2
ISB	2.0	0.2	0.5	0.9	0.2	0.6
Nucleon size	1.6	1.5	0.6	0.6	1.3	0.0
Relativistic	0.6	-	1.5	1.4	-	0.3
Coulomb	1.2	-	0.3	0.3	-	0.2
Multipole expansion	2.0	-	0.6	2.0	-	1.4
Higher $Z\alpha$	1.5	-	0.4	0.7	-	0.5
Magnetic MEC	0.4	-	0.1	0.3	-	0.2
Total	4.1%	2.3%	2.5%	3.6%	2.7%	2.7%

¹³ See Refs. [58, 59] and Refs. therein.

Appendix B: List of individual contributions to the nuclear polarization energy correction

Table S2. Nuclear structure corrections to the 2S-2P Lamb shift ΔE [meV] in $\mu^3\text{He}^+$ and $\mu^3\text{H}$, obtained with the AV18/UIX and χEFT nuclear potentials. The brackets show only the numerical error in the presented precision. See text for details regarding the individual terms.

		$\mu^3\text{He}^+$		$\mu^3\text{H}$	
		AV18/UIX	χEFT	AV18/UIX	χEFT
$\delta^{(0)}$	$\delta_{D1}^{(0)}$	-6.479(06)	-6.633(1)	-0.7669(6)	-0.7848(1)
	$\delta_L^{(0)}$	0.232(00)	0.240(0)	0.0285(0)	0.0296(0)
	$\delta_T^{(0)}$	-0.103(00)	-0.107(0)	-0.0128(0)	-0.0132(0)
	$\delta_C^{(0)}$	1.000(01)	1.020(3)	0.0718(1)	0.0732(0)
sum		-5.346(05)	-5.486(7)	-0.6788(5)	-0.6956(3)
	$\delta_M^{(0)}$	0.081(02)	0.047(0)	0.0101(3)	0.0058(0)
$\delta^{(1)}$	$\delta_{R3}^{(1)}$	-8.539(12)	-8.711(3)	-	-
	$\delta_{Z3}^{(1)}$	8.100(10)	8.327(3)	0.1778(0)	0.1844(0)
$\delta^{(2)}$	$\delta_{R^2}^{(2)}$	0.632(00)	0.654(3)	0.0199(0)	0.0206(2)
	$\delta_Q^{(2)}$	1.015(01)	1.038(0)	0.0344(0)	0.0358(0)
	$\delta_{D1D3}^{(2)}$	-0.841(00)	-0.862(0)	-0.0783(1)	-0.0811(1)
δ_{NS}	$\delta_{R1}^{(1)}$	-1.294(00)	-1.314(0)	0.0280(0)	0.0287(0)
	$\delta_{Z1}^{(1)}$	2.256(01)	2.291(0)	0.0453(0)	0.0463(0)
	$\delta_{NS}^{(2)}$	-0.179(00)	-0.185(0)	-0.0272(0)	-0.0282(0)
	δ_{pol}^A	-4.114(17)	-4.201(8)	-0.4688(6)	-0.4834(4)
	δ_{Zem}^A	-10.356(10)	-10.618(3)	-0.2232(0)	-0.2307(0)
	δ_{TPE}^A	-14.470(14)	-14.819(8)	-0.6920(6)	-0.7140(4)